# Dielectrophoretic Cell Capture on Polyester Membranes

Conni Hanke,[†,‡] Petra S. Dittrich,[‡] and Darwin R. Reyes*,[†]

[†]Semiconductor and Dimensional Metrology Division, Physical Measurement Laboratory, National Institute of Standards and Technology, 100 Bureau Drive, MS 8120, Gaithersburg, Maryland 20899, United States
[‡]Department of Chemistry and Applied Biosciences, ETH Zurich, Wolfgang-Pauli-Strasse 10, 8093 Zurich, Switzerland

**S** *Supporting Information*
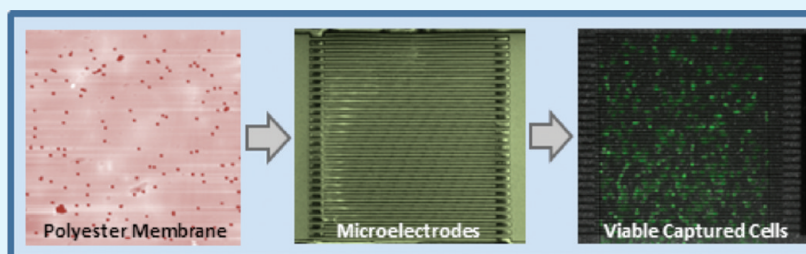


**ABSTRACT:** A new system for dielectrophoretic cell capture on permeable polyester membranes is presented. Conventional photolithographic techniques were used to fabricate gold microelectrodes on a polyester membrane. The characterization of the microelectrodes showed that there were no differences regarding roughness, permeability, and hydrophilicity of the membrane before and after processing. Finally, dielectrophoretic cell capture and viability in a microfluidic device was demonstrated on the patterned membrane. These membranes could ultimately be combined with multilayer microfluidic devices to form a powerful tool for studies of cell−cell interactions in coculture, whereby spatial separation of different cell types and/or microenvironments are required.

**KEYWORDS:** *permeable polyester (polyethylene terephthalate, PET) membrane, metallization, gold microelectrodes, dielectrophoresis, polyelectrolyte multilayer, cell capture, microfluidics*

## INTRODUCTION

The precise positioning of cells is a key requirement when dealing with microfluidic systems, specifically when cells are needed to be in defined areas for their stimulation and study. A number of approaches have been introduced to manipulate or capture cells within microchannels. They vary from mechanical traps[1,2] and flow control,[3,4] to optical[5,6] and electronic[7,8] techniques. Among the electronic techniques, dielectrophoresis (DEP) has gained a lot of attention in the microfluidics community. This phenomenon was first described by Pohl in 1951.[9] However, it was not until the past decade that the number of publications increased significantly for applications like biosensors,[10] medical diagnostics,[11] particle filtration,[12] nanoassembly,[13] and DNA manipulation.[14] The main advantages that DEP offers for particle manipulation include: label free entrapment, simplicity of instrumentation, favorable scaling effects, the ability to apply repulsive (negative DEP) and attractive (positive DEP) forces, and the lack of microfabricated obstacles that distort the flow within the channels.[15] DEP coupled with lab-on-a-chip devices have demonstrated suitability for DEP-based cell applications such as separation by size,[16,17] sorting,[18] focusing,[19] filtration,[20] trapping,[21,22] and patterning.[23,24]

In general, DEP electrodes have been patterned on solid substrates such as glass slides and silicon wafers. However, there are a few publications on patterning electrodes, for purposes other than DEP, onto permeable surfaces. For example, Duan and Meyerhoff showed that metallization of permeable membranes was possible and used patterned nylon membranes for sandwich enzyme immunoassays.[25] Later, Švorčík et al. characterized the sputtering process to metallize polyethylene terephthalate (PET, also referred to as polyester).[26] To the best of our knowledge, the patterning of gold microelectrodes on a permeable membrane has yet to be demonstrated. Furthermore, no dielectrophoretic manipulation has ever been shown on a material such as a permeable PET membrane.

We have previously used a multilayer microfluidic device with a PET membrane to separate the channels for cell culture and cell manipulation to monitor the induced gene expression of *ZsGreen1-DR*.[27] The use of permeable PET membranes in multilayer microfluidic devices has several advantages. Soluble factors could diffuse through the intermediate membrane, and their effect on the cells could be observed without disturbing influences caused by their supply. Additionally, the double-layered design adds another level of temporal and spatial control. The combination of a multilayer microsystem with dielectrophoretic cell capturing onto a permeable membrane

will enable in vitro coculture systems that could bring us closer to the cell—cell interactions that occur in vivo.

In this work, we present the fabrication, characterization, and use of a DEP microfluidic device comprised of gold microelectrodes on a permeable PET membrane. We used conventional photolithographic procedures along with other techniques to evaporate and lift-off gold on PET membranes to obtain patterns of interdigitated electrodes. These electrodes were characterized using atomic force microscopy (AFM), scanning electron microscopy (SEM), and optical microscopy. The electrodes were tested for dielectrophoretic cell capture, and cell viability on the gold and PET membrane surfaces.

## ■ EXPERIMENTAL SECTION

The PET membrane was first fixed onto a glass wafer using poly(methyl methacrylate) (PMMA) as adhesive, to prevent folding. Gold microelectrodes were fabricated on top of the PET membrane using conventional photolithographic and metallization techniques. The resulting microelectrodes were characterized by AFM, SEM, and optical microscopy. Polyelectrolyte multilayers (PEMs) were deposited onto the surface of the PET membrane containing the microelectrodes in order to trap and anchor cells. Subsequently, the microfluidic device was assembled and the microelectrodes were tested for cell capture by applying DEP forces. Cell viability was assessed 24 h after cell capture.

(Refer to the Supporting Information for a complete description and illustrations (Figure SI1 and SI2) of the experimental procedures.)

## ■ RESULTS AND DISCUSSION

**Characterization of the Gold/PET Surface.** We describe for the first time the fabrication of gold microelectrodes on a permeable PET membrane. The resulting DEP microelectrodes were characterized by several techniques. In Figure 1A a scheme of the gold pattern is shown. The interdigitated microelectrodes shown in the center are linked to contact pads. The micrograph in Figure 1B shows an actual gold/PET surface; the continuous connection of the patterned gold is visible. The pores of the PET membrane appear as black spots in the coated as well as uncoated areas of the surface. The SEM images show the surface (Figure 1C), and the insert (Figure 1D) of one single pore, used to characterize the gold deposition with respect to coverage or blockage of the micropores of the PET membrane. SEM imaging showed dark gray spots inside the pores, i.e., the gold did not completely block them. The average distance to which the gold was deposited inside the pores was 2.1 $\mu$m $\pm$ 1.2 $\mu$m. These observations suggest that the pores remained open and therefore permeable. Even if the partial blockage did slightly affect the function of the membrane where gold was deposited, half of the cell adhesion surface area was not covered by it. Therefore, the permeability of the membrane remained effectively unaffected.

In Figure 2, AFM micrographs of the membrane (A) before and (B) after processing are shown. The pores could be observed throughout the membrane regardless of the patterned gold. The coated areas within the pattern were continuously connected to result in interdigitated microelectrodes. In addition, the surface roughness of the PET membrane was measured before and after treatment to assess any possible changes during processing. An rms (root-mean-square) roughness of 28.7 nm $\pm$ 4.8 nm was observed for the membrane before processing, and an rms roughness of 24.3 nm $\pm$10.6 nm was observed after treatment. When these results were analyzed they showed no statistical difference (ANOVA, analysis of variance, single factor, $p = 0.33$). Even the rms roughness on
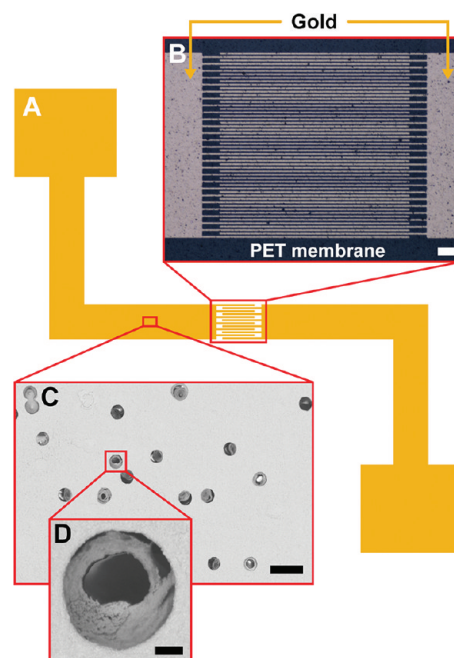


**Figure 1.** Scheme of the gold pattern and images of the gold patterned membrane. (A) The scheme shows the microelectrodes in the center, which are connected to contact pads. (B) Micrograph of the processed microelectrodes. (C) SEM image of the area used to measure the distance to which gold was deposited into the pores. The pores could be observed throughout the entire membrane. (D) Close up of one pore showing its partial blockage by the deposited gold. Scale bars: B, 100 $\mu$m; C, 3 $\mu$m; D, 300 nm.

the gold pattern (27.1 nm $\pm$ 9.6 nm) was not statistically different from the before and after processing values mentioned above ($p = 0.70$ and $p = 0.61$, respectively). The mechanical stability of the membrane was visually evaluated after processing, whereby no changes were detected.

Contact angle measurements were used to monitor the hydrophilicity of the membrane during the processing steps (see Table SI1 in the Supporting Information). With a water contact angle of 86° the membrane was slightly hydrophilic before any treatment. The sequential microfabrication steps decreased the contact angle to 69°, whereby the biggest change occurred after fixing the PET membrane onto the glass wafer via PMMA.

A multilayer microfluidic device (see Figure SI2 in the Supporting Information) was assembled to test the permeability of the PET membrane after processing. Two different food dyes were exchanged between the two layers by transporting them through the pores of the membrane (Figure 3 and the Supporting Information, Movie M1). This ultimately confirmed that its permeability was restored.

**DEP Cell Capture and Viability Assay.** The microelectrodes were tested for dielectrophoretic cell capture. In order to do this, a microfluidic device was assembled by placing a poly(dimethyl siloxane) (PDMS) microfluidic channel perpendicular to the microelectrodes (Figure 4).

For the cell trapping experiment, NIH-3T3 cells were harvested in low-conductive media (to perform positive DEP) and inserted into the microchannel, prefilled with the same media. To avoid cell damage, we carried out the dielectrophoretic cell capture within 5 min after harvesting the cells. We trapped cells in about half of the microelectrode surfaces by
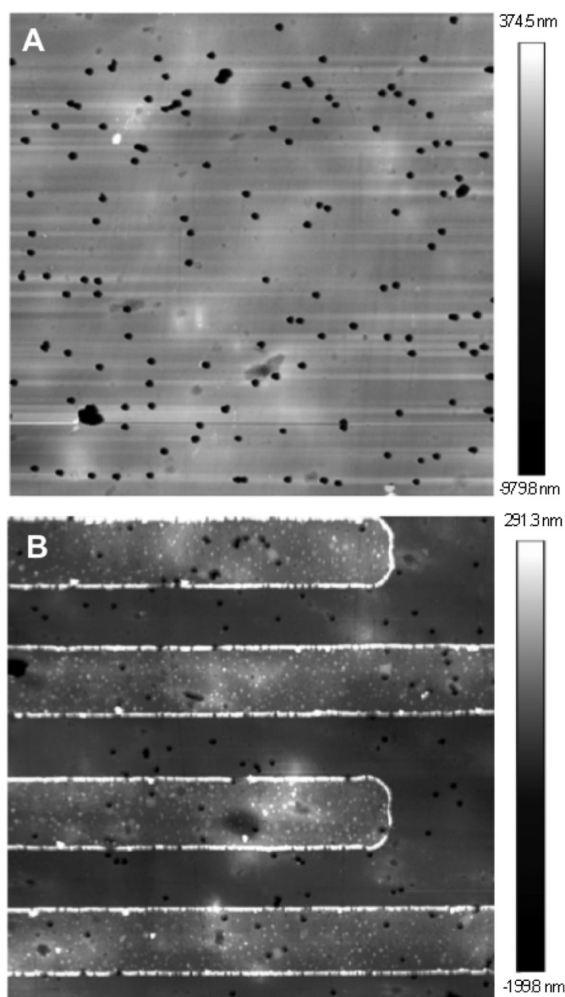
1879

dx.doi.org/10.1021/am300270k | ACS Appl. Mater. Interfaces 2012, 4, 1878−1882

**Figure 2.** AFM images of PET membranes before and after processing: (A) PET before processing, (B) with gold electrodes patterned. Both figures are 75 μm × 75 μm. The pores are randomly distributed and have an average diameter of 1.2 μm. The pores can be easily observed throughout the PET membrane, including where the continuous layer of gold had been deposited.
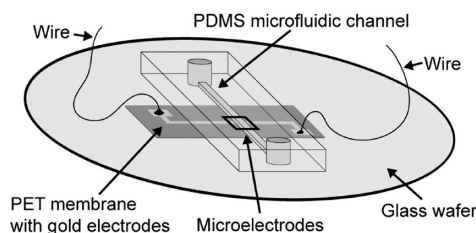


**Figure 4.** Sketch of the assembled microfluidic device. A piece of PET membrane with deposited gold electrodes was fixed onto a glass wafer. The precise location of the microelectrodes is indicated by the black square. The PDMS microfluidic channel was assembled on top, perpendicular to the microelectrodes. Wires were glued to the contact pads and connected to a waveform generator.

experienced higher electric fields, they were trapped on the first few electrodes. On the other hand, when lower electric fields were applied, cells tended to be trapped further down on the microelectrode array. The trapping efficiency could be increased further by either using a highly concentrated cell suspension or longer periods of DEP trapping. Additionally, the cell trapping efficiency can be influenced by the design of the microelectrodes.[28] By modifying the configuration of the electrodes, this could be further improved. Most of the trapped cells (approximately 90%) still remained on the PEMs after switching off the DEP forces and exchanging the low-conductive media with cell culture media. Cells attached well, as observed in Figure 5A. A live/dead assay was carried out 24 h after cell attachment. The assay showed that about 99% of the cells emitted green fluorescence; i.e., these cells were alive (Figure 5B). An influence of the material on cell adhesion and viability could be excluded because of similar cell behavior on various surfaces (see Figure SI3 in the Supporting Information).

DEP has been widely used in microfluidic platforms. The choice of platform will depend on the experiments to be carried out. The type of bioparticle (e.g., cells and viruses) to be manipulated defines guidelines such as the design of the electrodes or performing experiments with or without flow. For example, hematopoietic tumor cells were analyzed using a DEP system without applied flow. The electrodes generated cell trapping forces and at the same time created electrothermal vortices that produced efficient drug mixing, allowing for the analysis of cancer drug-induced cytotoxicity.[29] A similar

varying the applied voltage from 2 $V_{P-P}$ to 5 $V_{P-P}$ at a frequency of 10 MHz. Variations in the voltage allowed for cell capture across the length of the microelectrode array. When cells
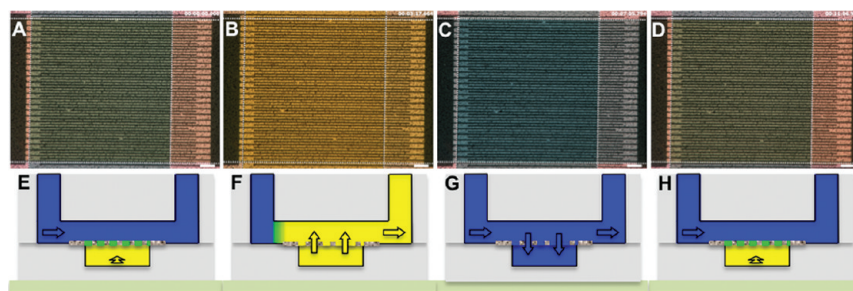


**Figure 3.** Permeability testing of the PET membrane after processing. (A–D) show actual images of yellow and blue food dyes exchanged between the channels in a multilayer microfluidic device by their transport through the pores of the PET membrane. The white dashed lines indicate the position of the two channels; the yellow dye flowed from left to right and the blue dye from top to bottom. (E–H) Corresponding sketches of the food dyes in the channels. (A, E) At *t* = 0, both flow rates were 0.5 μL/min, resulting in a green color at the crossing. (B, F) After changing the flow rates (yellow, 10 μL/min; blue, 0 μL/min), the yellow dye was transported to the top channel through the membrane and filled it (approximately *t* = 3 min). (C, G) After inverting the flow rates, the blue dye was transported to the bottom channel and filled it (approximately *t* = 7 min). (D, H) The green color returned after setting both flow rates back to 0.5 μL/min (approximately *t* = 11 min). Scale bars: 100 μm.
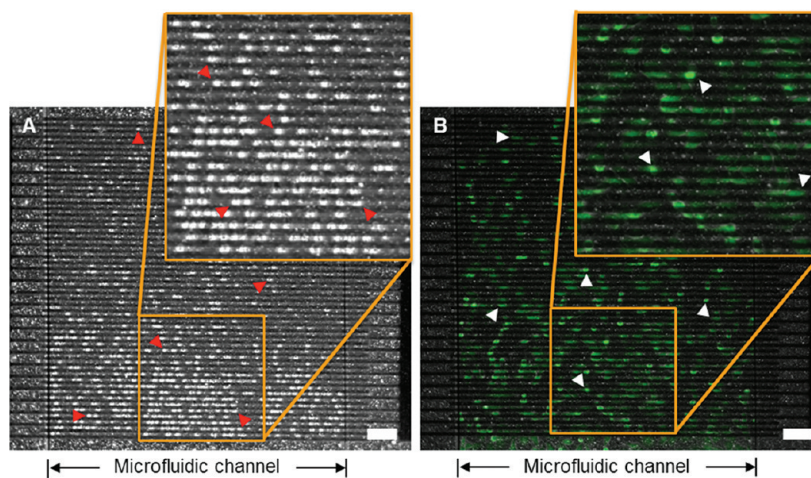
**Figure 5.** Efficient cell capture using DEP. (A) Micrograph after switching off DEP forces and exchanging low-conductive media with cell culture media (0 h). NIH-3T3 cell capture was evident, as soon as 5 min from the time the microelectrodes were energized. Cells flowed from bottom to top of the figure during DEP trapping. Red arrowheads point at some of the trapped cells. (B) A live/dead staining 24 h after cell capture was carried out. The cells spread onto the membrane and green fluorescence could be observed in approximately 99% of the cells, demonstrating that cells were viable. White arrowheads point to some of the viable cells. Inserts show some of the trapped cells in more detail. Scale bars: 100 $\mu$m.

experiment was carried out where hepatitis A viruses were trapped in a microsystem using electro-hydrodynamic flow and DEP forces.[30] These kinds of systems use nonadherent bioparticles and therefore provide platforms that can usually be reused several times. However, studies using adherent cells mostly require cell adhesive molecules on top of the electrodes to allow cell behavior and therefore cell responses that would provide meaningful data. Because cells tend to rearrange the adhesive molecules they attach onto and leave behind residues from their own extracellular matrix after detaching, the number of times the devices can be reused is limited. When cells are used in a microfluidic platform it is beneficial to have some form of trapping mechanism. However, the use of, for example, mechanical traps creates areas with different flow velocities, hence influencing the flow near the cells. This could likely affect the results of experiments in the cases where cells are sensitive to such shear forces. In contrast, DEP systems with planar electrodes render a channel without features that disturb the flow.

Our results demonstrate the functionality of the patterned microelectrodes on the permeable PET membrane for dielectrophoretic cell capture. This membrane along with DEP would be suited for specialized applications such as studies of drug transport, cell monolayer permeability and cell cocultures, among others. However, these applications would gain the most when combined with multilayer microfluidic devices. The added levels of control and the benefit of the localized cell enrichment by DEP trapping are at the heart of these devices. In addition, the combination of DEP and PEMs on a permeable PET membrane allows fast and reliable cell capture at a high efficiency, and hence subsequent long-term cell culture is achievable.

## CONCLUSION

For the first time, the use of gold microelectrodes on PET membranes as substrates to perform DEP cell entrapment in a microfluidic device is presented. The microelectrodes for DEP were fabricated using conventional photolithographic and metallization processes. We characterized the membrane with different techniques, and results showed that there was no

difference in terms of hydrophilicity, roughness, and permeability of the membrane when comparing the before and after processing surfaces. Finally, we showed that the patterned electrodes can be used for DEP cell trapping experiments in a microfluidic channel. The cell viability assessment showed that cells were viable 24 h after DEP trapping, demonstrating that long-term cell experiments can be carried out. This approach allows for an easy and rapid way of cell entrapment and enrichment onto PET membrane surfaces. By combining this work with multilayer microfluidic devices a new platform for cell−cell interactions or cell coculture studies could be developed. Cell exposure to different microenvironments would be possible, having two cell types physically separated. Future work will focus on the use of these membranes in multilayered microfluidic systems for cell−cell interaction studies.

## ASSOCIATED CONTENT

### Ⓢ Supporting Information

A complete description of the experimental procedures including figures describing the step-by-step fabrication of gold microelectrodes on PET membranes and the multilayer microfluidic device; additional results are also included in this section (PDF). SI-Movie M1 of dyes being exchanged between membranes (AVI). This material is available free of charge via the Internet at http://pubs.acs.org.

## AUTHOR INFORMATION

### Corresponding Author

*E-mail: darwin.reyes@nist.gov. Phone: 301-975-5466. Fax: 301-975-5668.

### Notes

The authors declare no competing financial interest.

## ACKNOWLEDGMENTS

## ■ REFERENCES

(1) Di Carlo, D.; Aghdam, N.; Lee, L. P. *Anal. Chem.* **2006**, *78*, 4925−4930.

(2) Ryley, J.; Pereira-Smith, O. M. *Yeast* **2006**, *23*, 1065−1073.

(3) Unger, M. A.; Chou, H. P.; Thorsen, T.; Scherer, A.; Quake, S. R. *Science* **2000**, *288*, 113−116.

(4) Shim, J.-U.; Olguin, L. F.; Whyte, G.; Scott, D.; Babtie, A.; Abell, C.; Huck, W. T. S.; Hollfelder, F. *J. Am. Chem. Soc.* **2009**, *131*, 15251−15256.

(5) Enger, J.; Goksör, M.; Ramser, K.; Hagberg, P.; Hanstorp, D. *Lab Chip* **2004**, *4*, 196−200.

(6) Dholakia, K.; Reecea, P.; Gu, M. *Chem. Soc. Rev.* **2008**, *37*, 42−55.

(7) Wang, X. J.; Wang, X. B.; Gascoyne, P. R. C. *J. Electrostatics* **1997**, *39*, 277−295.

(8) Huang, Y.; Wang, X. B.; Becker, F. F.; Gascoyne, P. R. C. *Biophys. J.* **1997**, *73*, 1118−1129.

(9) Pohl, H. A. *J. Appl. Phys.* **1951**, *22*, 869−871.

(10) Varshney, M.; Li, Y.; Srinivasan, B.; Tung, S. *Sens. Actuators, B* **2007**, *128*, 99−107.

(11) Srivastava, A. K.; Daggolu, P. R.; Burgess, S. C.; Minerick, A. R. *Electrophoresis* **2008**, *29*, 5033−5046.

(12) Gascoyne, P. R. C.; Vykoukal, V. *Electrophoresis* **2002**, *23*, 1973−1983.

(13) Hermanson, K. D.; Lumsdon, S. O.; Williams, J. P.; Kaler, E. W.; Velev, O. D. *Science* **2001**, *294*, 1082−1086.

(14) Asbury, C. L.; Diercks, A. H.; van den Engh, G. *Electrophoresis* **2002**, *23*, 2658−2666.

(15) Cetin, B.; Li, D. *Electrophoresis* **2011**, *32*, 2410−2427.

(16) Kang, K. H.; Kang, Y.; Xuan, X.; Li, D. *Electrophoresis* **2006**, *27*, 694−702.

(17) Kang, Y.; Li, D.; Kalams, S. A.; Eid, J. E. *Biomed. Microdevices* **2008**, *10*, 243−249.

(18) Hu, X.; Bessette, P. H.; Qian, J.; Meinhart, C. D.; Daugherty, P. S.; Soh, H. T. *Proc. Natl. Acad. Sci. U. S. A.* **2005**, *102*, 15757−15761.

(19) Church, C.; Zhu, J.; Wang, G.; Tzeng, T-R. J.; Xuan, X. *Biomicrofluidics* **2009**, *3*, 044109−1−044109−10.

(20) Cummings, E. B.; Singh, A. K. *Anal. Chem.* **2003**, *75*, 4724−4731.

(21) Asbury, C. L.; Diercks, A. H.; van den Engh, G. *Electrophoresis* **2002**, *23*, 2658−2666.

(22) Germishuizen, W. A.; Wälti, C.; Wirtz, R.; Johnston, M. B.; Pepper, M.; Davies, A. G.; Middelberg, A. P. J *Nanotechnology* **2003**, *14*, 896−902.

(23) Hsiung, L.-C.; Yang, C.-H.; Chiu, C.-L.; Chen, C.-L.; Wang, Y.; Lee, H.; Cheng, J.-Y.; Ho, M.-C.; Wo, A. M. *Biosens. Bioelectron.* **2008**, *24*, 869−875.

(24) Reyes, D. R.; Hong, J. S.; Elliott, J. T.; Gaitan, M. *Langmuir* **2011**, *27*, 10027−10034.

(25) Duan, C.; Meyerhoff, M. E. *Anal. Chem.* **1994**, *66*, 1369−1377.

(26) Švorčík, V.; Zehentner, J.; Rybka, V.; Slepička, P.; Hnatowicz, V. *Appl. Phys. A: Mater. Sci. Process* **2002**, *75*, 541−544.

(27) Hanke, C.; Waide, S.; Kettler, R.; Dittrich, P. S. *Anal. Bioanal. Chem.* **2012**, *402*, 2577−2585.

(28) Khoshmanesh, K.; Nahavandi, S.; Baratchi, S.; Mitchell, A.; Kalantar-Zadeh, K. *Biosens. Bioelectron.* **2011**, *26*, 1800−1814.

(29) Khoshmanesh, K.; Akagi, J.; Nahavandi, S.; Skommer, J.; Baratchi, S.; Cooper, J. M.; Kalantar-Zadeh, K.; Williams, D. E.; Wlodkowic, D. *Anal. Chem.* **2011**, *83*, 2133−2144.

(30) Grom, F.; Kentsch, J.; Müller, T.; Schnelle, T.; Stelzle, M. *Electrophoresis* **2006**, *27*, 1386−1393.